Inorganic Chemistry

Article

pubs.acs.org/IC

Cluster Harvesting by Successive Reduction of a Metal Halide with a Nonconventional Reduction Agent: A Benefit for the Exploration of Metal-Rich Halide Systems

Markus Ströbele, Agnieszka Mos, and Hans-Jürgen Meyer*

Section of Solid State and Theoretical Inorganic Chemistry, Department of Inorganic Chemistry, Auf der Morgenstelle 18, Eberhard Karls University Tübingen, D-72076 Tübingen, Germany

Supporting Information

ABSTRACT: The preparation of thermally labile compounds is a great temptation in chemistry which requires a careful selection of reaction media and reaction conditions. With a new scanning technique denoted here as *Cluster Harvesting*, a whole series of metal halide compounds is detected by differential thermal analysis (DTA) in fused silica tubes and structurally characterized by X-ray powder diffraction. Experiments of the reduction of tungsten hexahalides with elemental antimony and iron are presented. A cascade of six compounds is identified during the reduction with antimony, and five compounds or phases are monitored following the reduction with iron. The crystal structure of $Fe_2W_2Cl_{10}$ is reported, and two other phases in the Fe−W−Cl system are discussed.

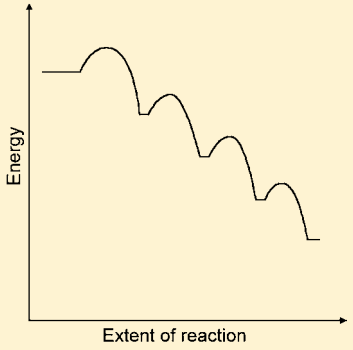

INTRODUCTION

Metal-rich halide cluster compounds are known for various group 3−7 metal halides (X = Cl, Br, I), most of them forming octahedral M_6X_{12} and M_6X_8 type structures.[1] The more electron poor group 4 metals are known to form interstitially stabilized octahedral M_6ZX_{12} type clusters.[2]

Preparations of metal-rich halide cluster compounds are usually performed by high-temperature solid state techniques. Reactions depart from a metal halide which is reduced by the same metal or by an effective reduction agent, such as an alkali metal or Al, in fused (silica glass, Nb, or Ta) ampules for several days at temperatures in excess of 700 °C.

Low-temperature syntheses for the preparation of thermally labile compounds have always been considered.[3] However, many transition metal elements such as molybdenum and tungsten behave inertly in solid state reactions at these conditions. Several strategies were explored to overcome this problem and to be able to perform kinetically controlled reactions. One proposition is the employment of a salt melt, which has been explored in several ways. The reaction of molybdenum halides in molten $AlCl_3$ containing the components KCl, $BiCl_3$, and elemental Bi as a reduction agent was reported many years ago.[4] A reduction of WCl_6 with Sn in the Lewis acidic ionic liquid [BMIM]Cl/$AlCl_3$ at room temperature was reported yielding $Sn(SnCl)[W_3Cl_{13}]$.[5] A solvothermal reduction of WCl_6 with As in CCl_4 was reported to yield a chlorocarbyne complex, $W_2Cl_7(CCl)$.[6] A comprehensive study of the binary W−I system is based on reactions of $W(CO)_6$ with iodine, which was successfully used to develop a large series of tungsten iodide cluster compounds, in which increasing cluster nuclearities were obtained with increasing temperature.[7] Separate explorations of this type of reaction have yielded the compound $W_{15}I_{47}$ and revealed this method as challenging with respect to the CO liberation inside the closed reaction vessel.[8]

Several years ago, a low-temperature reaction was introduced regarding the employment of nonconventional reduction agents used in the reduction of tungsten chloride.[9] One interesting example is the reduction of WCl_6 with elemental Bi which occurs at 350 °C.

More examples of the reduction of tungsten halides with the employment of reduction agents such as Sb, Fe, and Co are studied in our laboratory by differential thermal analyses (DTA). It turns out that these reactions involve a cascade of thermally metastable compounds until a stable product is formed (Figure 1). According to our experience, this type of investigation opens a new window for a systematic detection and for a rational synthesis of cluster compounds.

During our experiments, it turned out once more that the use of mild reaction conditions can bring up new interesting tungsten halide cluster compounds at temperatures as low as 200 °C. Even a cascade of compounds is discovered for systems when thermal effects of reactions are carefully controlled by applying a continuous heating rate. Hence, a differential thermal analysis can reveal a whole sequence of compounds when departing from just one starting composition of reaction partners, as we have demonstrated for the reduction studies of WX_6 (X = Cl, Br) with elemental antimony and iron.

Received: January 30, 2013
Published: May 29, 2013

   dx.doi.org/10.1021/ic4009366 | *Inorg. Chem.* 2013, 52, 6951−6956

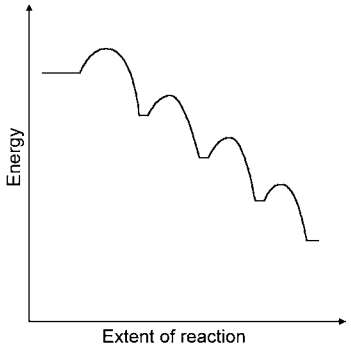

Figure 1. Exemplary scheme for a reaction of WCl_6 with a sufficient amount of a reduction agent, passing through several intermediate stages (compounds) with increasing temperature.

Here, we present DTA studies of two systems: The Sb−W−Br system has recently been investigated by using single attempt reactions at various temperatures with no less than three new compounds that have been reported. Here, we describe a DTA monitoring of this system, revealing the whole series of compounds, including the existence of one missing example, all being formed in one sequence of exothermic reactions.

The Fe−W−Cl system has not been fully explored. A thermal scanning indicates the formation of at least five compounds, of which two have been previously reported as FeW_2Cl_{10} and FeW_6Cl_{14}. The structure of the new compound $Fe_2W_2Cl_{10}$ is reported, and two other phases are discussed.

EXPERIMENTAL SECTION

Preparation and DTA. A mixture of WX_6 (X = Cl, Br; Aldrich, 99.9%; prepared according to ref 16) and the reduction agent (elemental antimony or iron powders) were combined in a molar ratio corresponding to the composition W_6X_{12} (plus the corresponding halide of the reduction agent) to allow a successive reduction of tungsten from the oxidation state +6 to +2. The starting mixture (200−250 mg) was loaded into a homemade silica sample holder under dry argon atmosphere (glovebox) and sealed under vacuum while cooling the sample with liquid N_2. The sealed sample holder and a reference container (Figure 2) were inserted into a differential thermal analyzer (STA 449 F3 Jupiter, Netzsch) and heated at a rate of 2 °C/min, while the thermal effects of the progressive reduction steps were monitored.

Crystalline samples useful for X-ray diffraction measurements are obtained when interrupting the DTA measurement at a certain temperature. Side phases ($SbBr_3$ or $FeCl_2$) were sublimed off or washed away with water. Separate reactions in fused silica ampules were used for the preparation of compounds by using tube furnaces, allowing for longer reaction durations, which can be useful to improve the crystal growth.

X-ray Diffraction. X-ray powder diffraction data were collected on a Stoe StadiP diffractometer using Ge-monochromatized Cu $K_{\alpha 1}$ radiation (Figure 5). Powder patterns of known compounds were assigned by pattern matching. This was the case for known products obtained from the reduction of WBr_6 with Sb. The powder pattern recorded for the hypothetical compound W_5Br_{12} contained several other phases and remains unattended here. A number of X-ray powder patterns were recorded and indexed for $W(Fe_x)Cl_6$ and $(Fe,W)Cl_2$ samples having varying nominal[10] iron contents, and lattice parameters were refined there by using the WinPlotr (FullProf)[11] program package. However, these phases deserve more detailed studies which will be done in a separate work. Here, we only present some lattice parameters for $W(Fe_x)Cl_6$ ($R\bar{3}$, a = 6.114(4), c = 16.786(8), V = 543.3(6) Å^3 for x = 0.1; a = 6.133(2) Å, c = 17.035(4) Å, V = 554.9(3) Å^3 for x = 0.75) and for $(Fe,W)Cl_2$ ($R\bar{3}$m, a = 3.3957(3) Å, c = 18.048(3) Å, V = 180.23(4) Å^3; a = 3.4063(3) Å, b = 18.082(4) Å, V = 181.69(4) Å^3, for nominal Fe/W ratios of 0.6:0.4 and 0.65:0.35). Powder patterns of these phases are contained in Figure 5, which show the presence of $FeCl_2$ ($R\bar{3}$m, a = 3.598 Å, c = 17.481 Å, V = 195.98 Å^3)[12] as a side phase of the reaction. The powder pattern of $(W,Fe)Cl_6$ contains $WOCl_4$ as another side phase (Figure 5), which sublimes off when samples are treated at higher temperatures.

Figure 2. Homemade silica containers placed on a DTA sample holder. One silica container is charged with a mixture of WCl_6 and a reduction agent; the other (empty) one serves as a reference container.

The WinPlotr (FullProf) program package was used for the structure refinement of $Fe_2W_2Cl_{10}$, with the final refinement pattern displayed in Figure 6. Iron positions in $Fe_2W_2Cl_{10}$ are refined with full occupancy. Data of the structure refinement are given in Table 1, and atom positions are listed in Table 2.

Table 1. Structure Refinement of $Fe_2W_2Cl_{10}$ from X-ray Powder Data

chemical formula	$Fe_2W_2Cl_{10}$
formula weight, g/mol	833.88
temperature, K	298(2)
crystal system	monoclinic
space group	$C\,2/c$ (No. 15)
a, Å	6.2486(4)
b, Å	16.734(1)
c, Å	12.637(1)
β, °	109.713(4)
V, Å^3	1244.0(2)
Z	4
$d_{calc.}$, g/cm^3	4.452
Θ range for data collection, °	5.5−45
total number of reflections	549
refined parameters	40
R_p, R_{wp}	2.324, 3.073
R_{Bragg}	9.441
χ^2	3.987
λ, Å	1.5406
μ, mm^{-1}	71.063

dx.doi.org/10.1021/ic4009366 | Inorg. Chem. 2013, 52, 6951−6956

Table 2. Atom Positions and Isotropic Equivalent Displacement Parameters (Å^2) in the Crystal Structure of $Fe_2W_2Cl_{10}$

	Wyckoff site	x	y	z	U_{eq}[a]
W(1)	4e	0	0.82235(4)	1/4	0.0344(4)
W(2)	4e	0	0.97993(5)	1/4	0.0453(4)
Fe(1)	4e	0	0.2020(2)	1/4	0.0338(8)
Fe(2)	4e	0	0.5826(2)	1/4	0.074(1)
Cl(1)	8f	0.2463(3)	0.1007(2)	0.9015(1)	0.0152(3)
Cl(2)	8f	0.2792(4)	0.1960(1)	0.6510(2)	0.0152(3)
Cl(3)	8f	0.2091(3)	0.0100(1)	0.6151(2)	0.0152(3)
Cl(4)	8f	0.2267(2)	0.3029(1)	0.8370(2)	0.0152(3)
Cl(5)	8f	0.2572(3)	0.9149(1)	0.8649(1)	0.0152(3)

[a]Displacement parameters of chloride ions were restrained to be equivalent.

RESULTS AND DISCUSSION

Thermal studies on tungsten hexachloride have been previously performed, showing the formation of eutectics with tungsten tetrachloride and other metal halides, without a focus on reducing conditions.[13] A classical way for the reduction of WCl_6 is the employment of aluminum powder to obtain WCl_4 (at 370 °C), which undergoes a disproportionation reaction to yield W_6Cl_{12} (around 470 °C).[14]

Our present studies are designed to systematically detect (DTA) and to investigate (XRD) compounds of a given system that appear during the successive reduction of tungsten hexahalide. The DTA experiments and the preparations are performed under similar conditions in fused silica tubes, whereas separate reactions appear useful when longer reaction times are desired.

DTA Studies. *The Sb–W–Br System.* The reduction of WBr_6 with elemental antimony was performed according to the nominal reaction:

$$6WBr_6 + 8Sb \rightarrow W_6Br_{12} + 8SbBr_3$$

The starting mixture was fused into a silica container and heated in a DTA apparatus with the resulting thermogram displayed in Figure 3. This experiment demonstrates that all previously reported compounds in the Sb–W–Br system can be detected by their heats of formation.

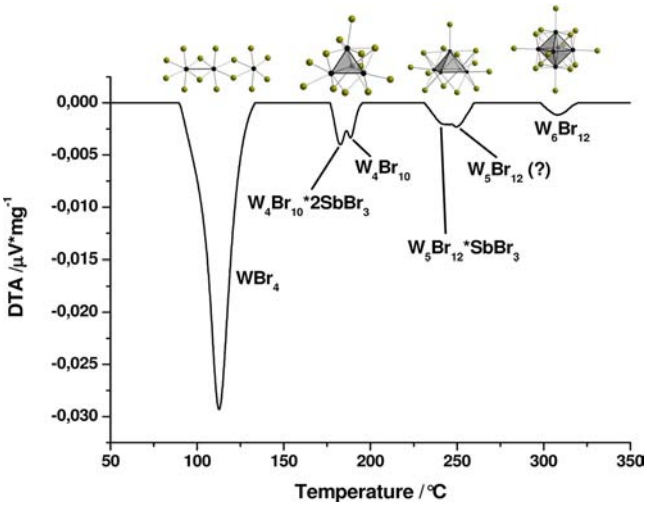

Figure 3. Exothermic effects during the reduction of WBr_6 with elemental Sb at increasing temperature and cluster motifs formed during the reaction cascade (top).

The DTA pattern of the reaction of WBr_6 with elemental Sb displays exothermic effects related to the formation of several compounds, which were separately identified by X-ray powder diffraction. The first signal refers to the formation of WBr_4,[6] followed by two closely adjacent signals representing the formation of $W_4Br_{10}{\cdot}2SbBr_3$ and W_4Br_{10}.[5] Another double signal appears near 250 °C of which one compound is assigned as $W_5Br_{12}{\cdot}SbBr_3$.[6] The second compound, which is not yet characterized, we assume as binary W_5Br_{12}. Finally, W_6Br_{12} is formed above 300 °C. During the reaction progress, large crystals of $SbBr_3$ were growing in the silica container.

This study represents an example for the investigation of the binary tungsten bromide system including some $SbBr_3$ adducts with tetrahedral,[15] square pyramidal,[16] and octahedral[17] metal atom cores. It can be seen that smaller clusters behave thermally labile, showing increasing cluster nuclearities and the conversion into an octahedral cluster with increasing temperature.

The Fe–W–Cl System. The reduction of WCl_6 with iron powder was performed according to the nominal reaction:

$$6WCl_6 + 12Fe \rightarrow FeW_6Cl_{14} + 11FeCl_2$$

The starting mixture was fused into a silica container and heated in a DTA apparatus with the resulting differential thermogram displayed in Figure 4. X-ray powder patterns assigned to all exothermic events, which were detected in the DTA, are displayed in Figure 5.

Trigonal WCl_6[18] was used as a starting material for the reaction with elemental iron powder. The first exothermic effect

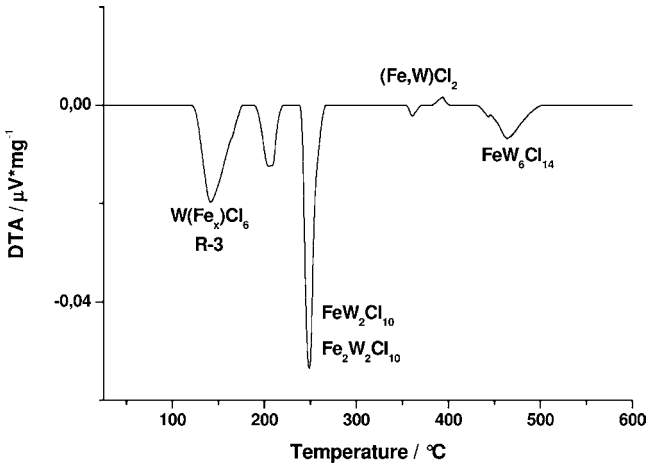

Figure 4. Thermal effects during the reduction of WCl_6 with Fe powder at increasing temperature.

dx.doi.org/10.1021/ic4009366 | Inorg. Chem. 2013, 52, 6951–6956

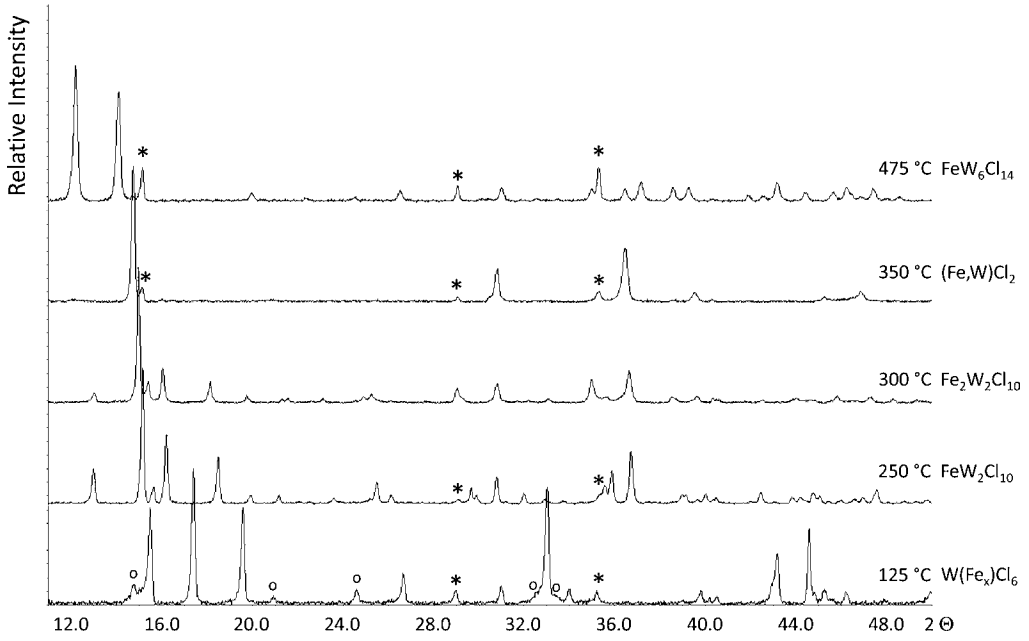

Figure 5. X-ray powder patterns of compounds obtained during the reduction of WCl_6 with Fe powder at certain reaction temperatures (given in the figure). Side phases are marked for $FeCl_2$ (∗) and $WOCl_4$ (o).

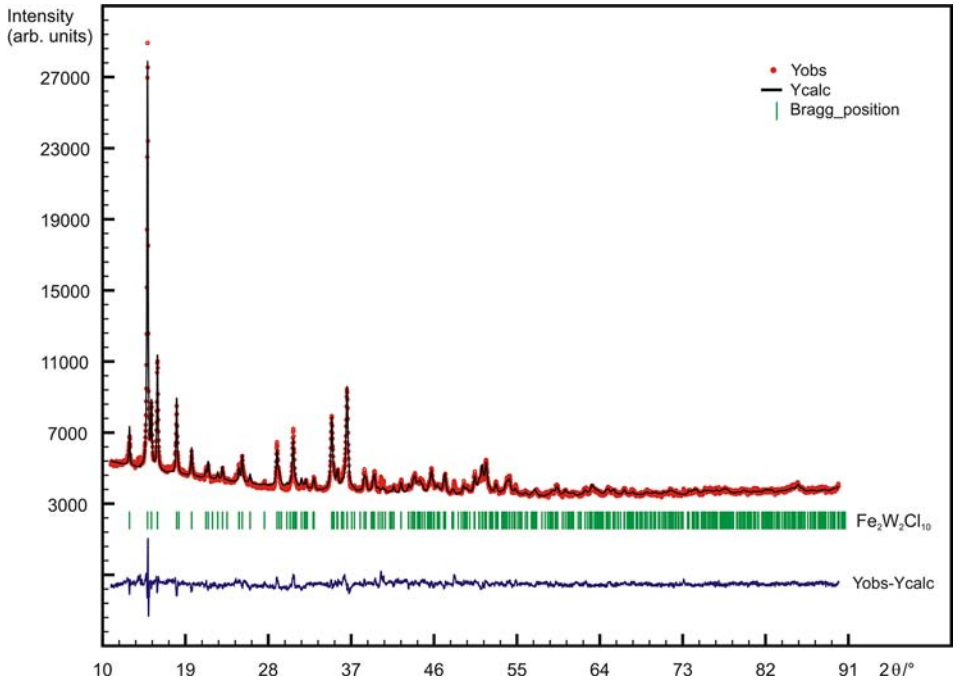

Figure 6. Structure refinement of $Fe_2W_2Cl_{10}$ based on X-ray powder data. Circles represent measured data; the calculated pattern is superimposed with the observed pattern (red). Ticks mark the Bragg reflections (green) of $Fe_2W_2Cl_{10}$ (coproduced $FeCl_2$ was sublimed off). The difference curve between the observed and calculated pattern is shown in the lower part of the graph (blue).

represents the (irreversible) formation of a structure that corresponds to rhombohedral *WCl*$_6$,[19] according to the assignment of the X-ray powder pattern. The following two exothermic effects displayed in the DTA are explained with the formation of FeW_2Cl_{10}[20] and an unknown compound that later turned out to be $Fe_2W_2Cl_{10}$ (see below). It can be seen in Figure 7 that the relatively open layer structure of FeW_2Cl_{10} adopts another Fe ion into its structure to form $Fe_2W_2Cl_{10}$. The next exothermic effect in the DTA corresponds to the formation a $CdCl_2$ type structure, according to X-ray diffraction data, which may be assumed as $(Fe,W)Cl_2$. This structure can be envisioned to be generated by occupying the remaining octahedral void in the structure of $Fe_2W_2Cl_{10}$ (Figure 7, at right) to yield the hypothetical formula *Fe*$_3$*W*$_2$*Cl*$_{10}$.

Right above the temperature related to the exothermic formation of the $CdCl_2$ type structure, a weak endothermic effect is obtained, slightly below 400 °C. It is not yet clear if this effect represents the breakdown of the $CdCl_2$ type structure or if another effect has to be assigned here. We note that all

dx.doi.org/10.1021/ic4009366 | *Inorg. Chem.* 2013, 52, 6951−6956

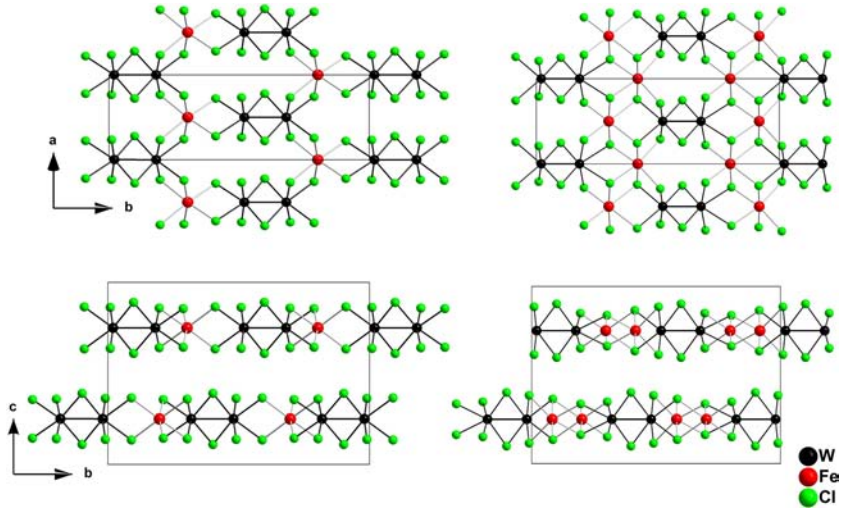

Figure 7. Crystal structures of FeW_2Cl_{10} (left) and $Fe_2W_2Cl_{10}$ (right). The top projections represent one layer, and the bottom projections display two layers, rotated by 90° around the (horizontal) *b*-axis.

previous structures are based on hcp and ccp (CdI_2 type) packing arrangements of chloride ions.

The final occasion recorded in the DTA represents the exothermic formation of $Fe[W_6Cl_{14}]$, which crystallizes isotypically with the $Pb[Mo_6Cl_{14}]$ type structure. The formation of this structure requires some rearrangement of ions in the structure, to achieve the formation of $(M_6X_8^i)X_6^a$ (i = inner, a = apical) type clusters.

Structural Studies. *$W(Fe_x)Cl_6$.* Two modifications have been reported for WCl_6. Our reactions departed from trigonal (β-)WCl_6 which transformed into rhombohedral *(α-)WCl_6* in the presence of iron powder around 140 °C. It was interesting to note that the obtained (rhombohedral) *WCl_6* behaved stable in air for many hours, in contrast to trigonal WCl_6 which immediately undergoes a hydrolysis reaction in air. Both structures are based on a hexagonal closest packing of chloride ions with different arrangements of tungsten ions occupying (1/6) of octahedral interstices. In order to investigate the role of iron in this reaction, separate experiments were carried out in fused silica tubes. Trigonal WCl_6 was reacted with increasing amounts of iron powder with the nominal composition $W(Fe_x)Cl_6$ with x = 0–0.75 for 600 h (at 125 and 140 °C). Trigonal WCl_6 with x = 0 remained the same after the heating procedure, according to XRD. For products with x > 0, a structural change into the rhombohedral *(α-)WCl_6* structure type occurred. The employment of an increasing amount of iron powder revealed an increase of lattice parameters corresponding to a unit cell volume expansion in the order of 12 $Å^3$ (for samples we have prepared so far).

These results are leading to the assumption of a variable intercalation of iron into the structure of WCl_6. The formula of this compound is $W(Fe_x)Cl_6$ if we assume that no tungsten is removed from the original WCl_6 structure during the reaction with iron powder. The phase width of $W(Fe_x)Cl_6$ remains unknown. More studies will be necessary to clarify the nature of this phase in detail.

Previously, an intercalation of lithium ions into the structure of WCl_6 has led to the formation of $LiWCl_6$.[21] Hence, this type of intercalation into WCl_6 can be regarded as an initial reduction step for WCl_6.

$Fe_2W_2Cl_{10}$. Powders of $Fe_2W_2Cl_{10}$ behave stable in air. The crystal structure of $Fe_2W_2Cl_{10}$, as refined from X-ray powder data (Figure 6), is closely related to the already reported structure of FeW_2Cl_{10}. Both structures are composed of a distorted hexagonal closest packed arrangement of chloride ions alternating along the *c*-axis direction (Figure 7, bottom). Metal atoms occupy octahedral interstices in every second interlayer at z = 1/4 and 3/4. One-fifth of octahedral positions are occupied by pairs of tungsten atoms which are moved toward each other to yield short interatomic distances which can be interpreted as bonding W–W interactions. Interatomic distances (d_{W-W} = 2.637(1) Å) calculated for $Fe_2W_2Cl_{10}$ are clearly shorter than the corresponding (d_{W-W} = 2.707(5) Å) distances reported for FeW_2Cl_{10}. The motif of an edge-sharing $[W_2Cl_{10}]$ double octahedron contained in these structures corresponds to a section of the WCl_4 structure, having a separation of tungsten atoms d_{W-W} = 2.688(2) Å[22] and 2.713(3) Å,[23] as reported from two different sources. Thus, W–W distances around 2.7 Å obtained for FeW_2Cl_{10} and WCl_4 may be typically addressed with an oxidation state of +4 for tungsten. The corresponding distance in $Fe_2W_2Cl_{10}$ appears shorter and should be addressed to a lower oxidation state (formally +3) of tungsten.

Two iron ions per formula unit $Fe_2W_2Cl_{10}$ occupy another one-fifth of octahedral sites. Metal–halide distances range at d_{W-Cl} = 2.388(2)–2.560(2) Å ($\overline{d}_{W-Cl}$ = 2.471(2) Å) and d_{Fe-Cl} = 2.284(3)–2.536(3) Å. The average Fe–Cl distance $\overline{d}_{W-Cl}$ = 2.440(3) Å in the structure of $Fe_2W_2Cl_{10}$ is in-between the corresponding average distances obtained in $FeCl_2$ (2.500(5) Å) and $FeCl_3$ (2.377(5) Å).

$(Fe,W)Cl_2$. The phase which we describe here as $(Fe,W)Cl_2$ appears as a dark-green, almost black powder. The X-ray powder pattern can be indexed isotypically to the crystal structure of $FeCl_2$. Until now, it is not known if this phase exhibits a cation deficiency. Calculated lattice parameters obtained from samples, prepared with different amounts of iron powder, (at 350 °C, 5 h) indicate the existence of a phase width. Lattice parameters calculated for $(Fe,W)Cl_2$ revealed a shorter *a*-axis and a longer *c*-axis compared to $FeCl_2$ and a smaller unit cell volume of $(Fe,W)Cl_2$. The strongest (003) X-ray reflection of the $FeCl_2$ side phase, indicated as (∗) in Figure 5, appears as a small peak right next to the corresponding strongest reflection of $(Fe,W)Cl_2$. A comparison of average Fe–Cl and W–Cl distances (2.440(3) and 2.471(2) Å) suggest

dx.doi.org/10.1021/ic4009366 | *Inorg. Chem.* 2013, 52, 6951–6956

quite similar radii for Fe and W ions in $Fe_2W_2Cl_{10}$. It is clear that more studies will be necessary to identify the composition and phase range of this structure.

CONCLUSION AND OUTLOOK

Thermally metastable compounds can be assumed to represent the largest group of yet missing compounds. For their discovery, soft reaction conditions allowing for kinetic control of the cluster formation seems to be a promising way. However, the temperature interval of the existence of a given compound can be very tight (see Figure 3), so that many missing compounds are discovered only under fortuitous reaction conditions. With the DTA monitoring approach presented herein, some binary W−Br and ternary M−W−Cl systems were successfully explored, allowing a whole series of compounds that can be harvested by combined DTA monitoring and preparations at corresponding temperatures.

It could be shown that compounds in the W−Br system can be monitored by their formation heats under successive reduction with antimony in fused silica ampules during one DTA run. Structural assignments for each compound were made by powder XRD, showing up the cluster nucleation process following the sequence binuclear, tetrahedral, square pyramidal, and octahedral. The Fe−W−Cl system was studied in a similar way. The reaction begins with the intercalation of iron ions into the hcp based structure of WCl_6 with the formation of $W(Fe_x)Cl_6$. In the following steps, FeW_2Cl_{10} and $Fe_2W_2Cl_{10}$ are formed, whose structures also based on hcp of chloride ions, where iron ions are incorporated into octahedral voids. With the hypothetical formula $Fe_3W_2Cl_{10}$, all octahedral sites in one layer are occupied, corresponding to a defect CdI_2 type structure. However, the next reaction step involves a structural change to a cubic closest packing arrangement of anions with the formation of $(Fe,W)Cl_2$, which is characterized by a defect $FeCl_2$ ($CdCl_2$) type structure. Finally, it can be assumed that $(Fe,W)Cl_2$ releases iron chloride to allow the formation of FeW_6Cl_{14}.

These exemplary studies performed for some tungsten halide compounds raise potential for a comprehensive investigation of the large field of ternary tungsten halide compounds and to gain a better understanding on transformation reactions. In addition, this procedure can be most likely applied to the development of several transition metal halide systems,[24] if not for the exploration of other systems. Behind this development of new compounds, there is always hope to find unusual or enhanced chemical or physical behavior.

ASSOCIATED CONTENT

Supporting Information

X-ray crystallographic information for $Fe_2W_2Cl_{10}$ in CIF format. This material is available free of charge via the Internet at http://pubs.acs.org.

AUTHOR INFORMATION

Corresponding Author

*E-mail: juergen.meyer@uni-tuebingen.de.

Notes

The authors declare no competing financial interest.

REFERENCES

(1) Welch, E. J.; Long, J. R. *Prog. Inorg. Chem.* **2005**, *54*, 1−45.
(2) Corbett, J. D. *J. Chem. Soc., Dalton Trans.* **1996**, 575−587.
(3) Osters, O.; Nilges, T.; Bachhuber, F.; Pielnhofer, F.; Weihrich, R.; Schönneich, M.; Schmidt, P. *Angew. Chem., Int. Ed.* **2012**, *51*, 2994−2997.
(4) Jödden, K.; Schäfer, H. *Z. Anorg. Allg. Chem.* **1977**, *430*, 5−22.
(5) Ahmed, E.; Groh, M.; Ruck, M. *Eur. J. Inorg. Chem.* **2010**, *33*, 5294−5297.
(6) Beck, J.; Wolf, F. *Z. Anorg. Allg. Chem.* **2002**, *628*, 1453−1454.
(7) Franolic, J. D.; Long, J. R.; Holm, R. H. *J. Am. Chem. Soc.* **1995**, *117*, 8139−8153.
(8) Ströbele, M.; Meyer, H.-J. *Z. Anorg. Allg. Chem.* **2010**, *636*, 62−66.
(9) Kolesnichenko, V.; Messerle, L. *Inorg. Chem.* **1998**, *37*, 3660−3663.
(10) It is clear that the given nominal composition does not reflect the true composition of a phase, as there may be some iron powder left over in the reaction.
(11) Roisnel, T.; Rodriguez-Carvajal, J. WinPLOTR: A Windows tool for powder diffraction patterns analysis, *Proceedings of the Seventh European Powder Diffraction Conference (EPDIC7)*, Barcelona, Spain, May 20−23, 2000; Delhez, R., Mittenmeijer, E. J., Eds.; Scitec Publications, Ltd.: Zurich, 2001; Vol. *118*.
(12) Vettier, C.; Yelon, W. B. *J. Phys. Chem. Solids* **1975**, *26*, 401−405.
(13) (a) Eliseev, S. S.; Malysheva, L. E.; Vozhdaeva, E. E.; Gaidenko, N. V. *Geol. Khim. Nauk.* **1978**, *4*, 129−132. (b) Drobot, D. V.; Nikolaev, A. V. Z. *Neorg. Khim.* **1977**, *22*, 2248−2250. (c) Chikanov, N. D. *Khim. Khim. Tekhnol.* **1970**, *13*, 1047−1049. (d) Korshunov, B. G.; Bezuevskaya, V. N. Z. *Neorg. Khim.* **1967**, *12*, 3280−3282.
(14) McCarley, R. E.; Brown, T. M. *Inorg. Chem.* **1964**, *3*, 1232−1236.
(15) Ströbele, M.; Meyer, H.-J. *Z. Anorg. Allg. Chem.* **2012**, *638*, 945−949.
(16) Ströbele, M.; Meyer, H.-J. *Russ. J. Coord. Chem.* **2012**, *38*, 178−182.
(17) Schäfer, H.; Siepmann, R. *Z. Anorg. Allg. Chem.* **1968**, *357*, 273−289.
(18) Taylor, J. C.; Wilson, P. W. *Acta Crystallogr.* **1974**, *B30*, 1216−1220.
(19) Ketlaar, J. A. A.; van Oosterhout, G. W. *Recl. Trav. Chim. Pays-Bas* **1943**, *62*, 197−200.
(20) Ströbele, M.; Meyer, H.-J. *Z. Anorg. Allg. Chem.* **2011**, *637*, 1024−1029.
(21) Weisser, M.; Tragl, S.; Meyer, H.-J. *Z. Kristallogr. NCS* **2007**, *223*, 5−6.
(22) Kolesnichenko, V.; Swenson, D. C.; Messerle, L. *Inorg. Chem.* **1998**, *37*, 3257−3262.
(23) Nägele, A. Synthese und Untersuchung von Clusterverbindungen der Übergangsmetalle Mo, W und Nb; Reaktivität bei Festkörperreaktionen, Dissertation, University Tübingen, Tübingen, Germany, 2001.
(24) Hay, D. N.; Swenson, D. C.; Messerle, L. *Inorg. Chem.* **2002**, *41*, 4700−4707.